Electronic Supplementary Information

Three-color Polymorph-dependent Luminescence: Crystallographic Analysis and Theoretical Study on Excited-state Intramolecular Proton Transfer (ESIPT) Luminescence of Cyano-substituted Imidazo[1,2-*a*]pyridine

Toshiki Mutai,*[,1] Hideaki Shono,[1] Yasuhiro Shigemitsu[2,3] and Koji Araki*[,1]

1. *Department of Materials and Environmental Science, Institute of Industrial Science, the University of Tokyo, 4-6-1, Komaba, Meguro-ku, Tokyo 153-8505, Japan*
2. *Industrial Technology Center of Nagasaki, 2-1303-8 Ikeda, Omura, Nagasaki 856-0026, Japan*
3. *Graduate School of Engineering, Nagasaki University, 1-14, Bunkyo-machi, Nagasaki 852-8521, Japan*

E-mail: araki@iis.u-tokyo.ac.jp, *mutai@iis.u-tokyo.ac.jp*

X-ray crystallographic data

X-ray diffraction data of the polymorphic crystals was collected on a Rigaku Mercury-CCD diffractometer equipped with a graphite-monochromatized Mo *K*α source (λ = 0.71070 Å) at 113 K. Data was processed using the CrystalClear program package and corrected for absorption. The structure was solved by direct method, SHELXS-97,[1] and expanded by subsequent Fourier synthesis. Refinement by full matrix least-squares calculations was performed using SHELXL-97.

Table S1. Crystallographic data and structure refinement summary.[a]

	2-Y	**2-O**	**2-R**
CCDC number[b]	965203	965204	965205
Molecular formula	$C_{14}H_9N_3O$	$C_{14}H_9N_3O$	$C_{14}H_9N_3O$
Molecular weight	235.24	235.24	235.24
Crystal size / mm^3	0.20 × 0.15 × 0.05	0.40 × 0.25 × 0.10	0.40 × 0.25 × 0.15
Crystal system	Monoclinic	Monoclinic	Monoclinic
Space group	$P2_1/n$	$P2_1/n$	$P2_1/n$
a / Å	6.052(6)	13.654(6)	3.8196(10)
b / Å	4.919(5)	7.343(3)	11.356(3)
c / Å	36.98(3)	14.200(6)	25.246(7)
β / deg.	94.115(4)	130.054(2)	93.1961(11)
V / Å^3	1098.0(17)	1089.8(8)	1093.3(5)
Z	4	4	4
$d_{calc.}$ / g cm^{-3}	1.423	1.434	1.429
μ / mm^{-1}.	0.094	0.095	0.094
λ / nm	0.71075	0.71075	0.71075
Temperature / K	113(2)	113(2)	113(2)
$2\theta_{max}$ / deg.	54.88	54.92	54.92
F_{000}	488	488	488
Measured/independent reflections	8137/2402	8291/2487	8368/2479
N_{para}	200	200	200
GOF	0.938	1.097	0.929
R_{int}	0.101	0.0267	0.110
R_1	0.0754	0.0334	0.0591
wR_2 (all data)	0.2201	0.0963	0.1328
Max/min residual electron density	0.312/-0.326	0.293/-0.197	0.364/-0.331

[a,b] These data can be obtained free of charge from The Cambridge Crystallographic Data Centre via *www.ccdc.cam.ac.uk/data_request/cif*.

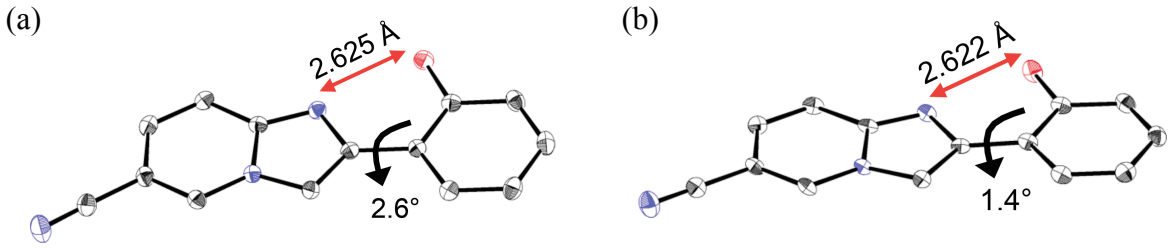

Figure S1. ORTEP drawings of **2-O** (a) and **2-R** (b).

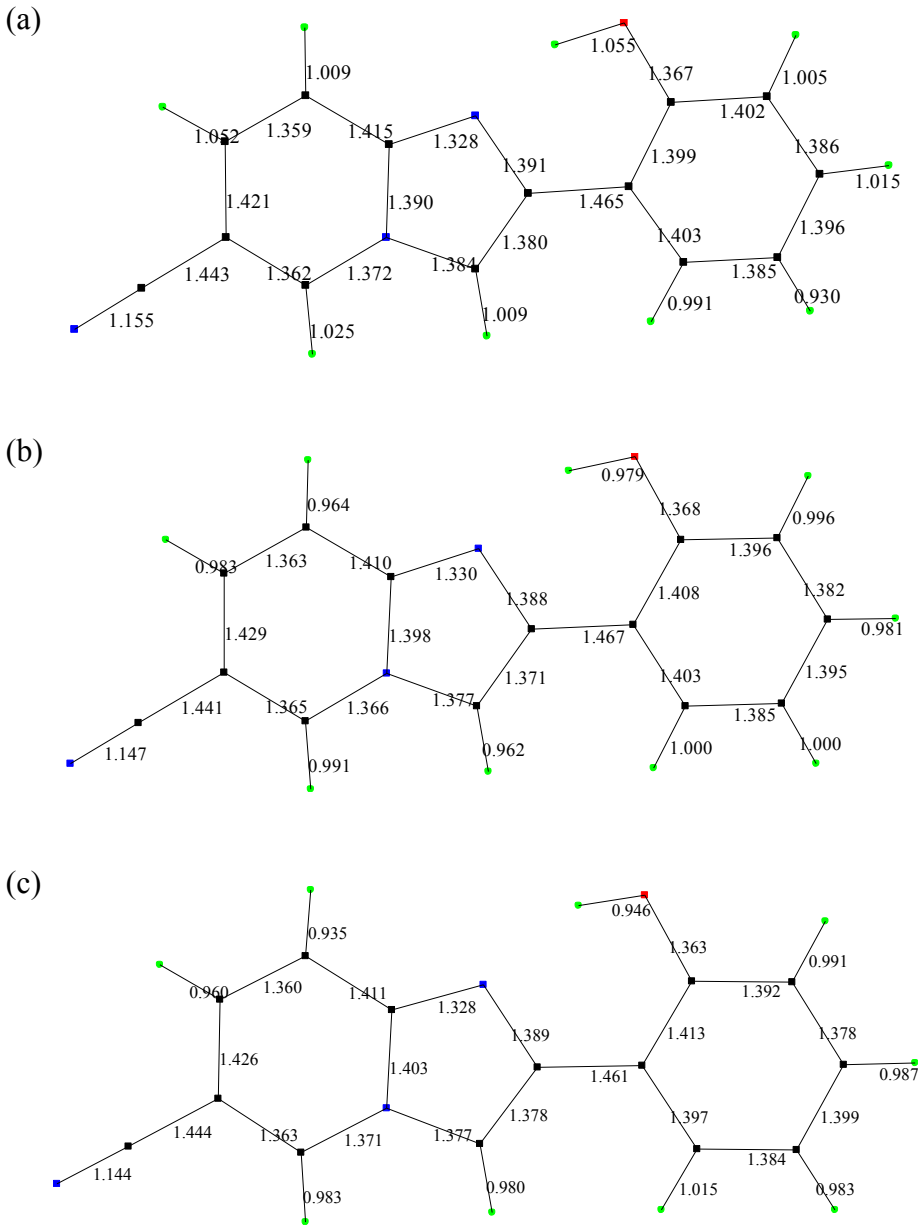

Figure S2. Bond lengths (Å) in a molecule **2** in the crystals **2-Y** (a), **2-O** (b) and **2-R**

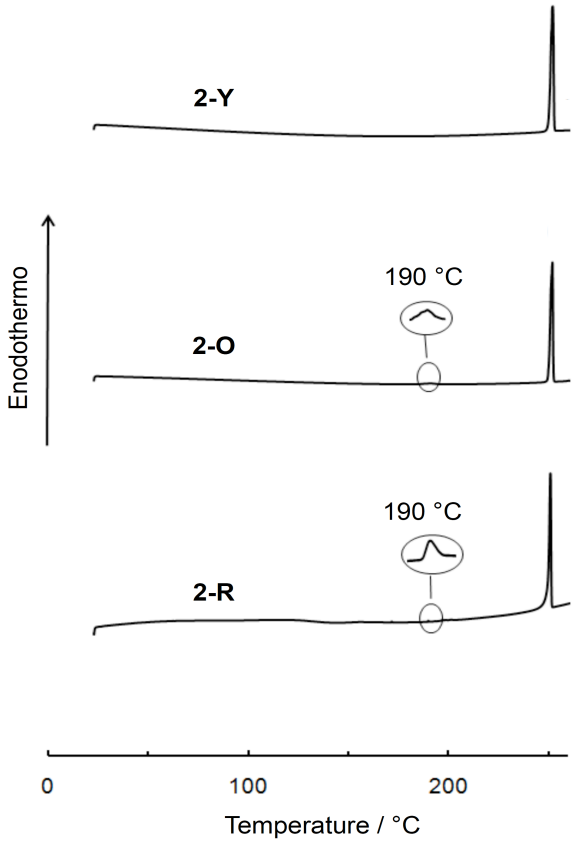

Figure S3. DSC curves of the crystals of **2-Y**, **2-O**, and **2-R**.

Computational details

Validation of the prediction accuracies of TDDFT calculation

For the isolated 6CN-NPIP in the S_1 state, geometry optimizations were carried out using TDDFT(B3LYP)/6-31+G(d), 4 state-averaged(SA)-CASSCF(8,8)/ANO-L in vacuo, respectively. The CASSCF calculations include near-frontier π orbitals (HOMO-3 to HOMO and LUMO to LUMO+3). The structures corresponding to the local minima were confirmed by harmonic frequency analysis. The S_1–S_0 energies were evaluated by TDDFT/6-31+G(d) level with two XC-functionals, i.e., B3LYP and its Coulomb-attenuated variant CAM-B3LYP.[2] CASSCF(10e,10o)/ANO-L and MS-CASPT2(10e,10o)/ANO-L level of theory were also employed where the extended active spaces include HOMO-5 n-orbitals and the two π virtual orbitals to include the n-π* mixing in a balanced way. The 4 SA-CASSCF(10e,10o) calculations were done and the 4 single-state (SS)-CASPT2(10e,10o) states were further averaged within MS-CASPT2 scheme. The level shift technique with careful choice of shift value (0.3) seems to work well with the fairly large reference weight of the main configuration. The Atomic Natural Orbitals large sets (ANO-L: C,N,O[4s3p2d]/H[3s2p]) were employed throughout the present study. The S_1 character was verified by all the calculation methods to possess overwhelming HOMO–LUMO excitation

coefficients. Table S2 shows that the energy gaps calculated by MS-CASPT2//CASSCF and MS-CASPT2//TDDFT were similar, indicating that the TDDFT(B3LYP)/6-31+G(d) level optimization was sufficient to obtain an appropriate geometry of **2** for further discussion. Modern TD-DFT methods have been confirmed to achieve excellent performance that is compatible with more computationally demanding, wavefunction-based methods.[3,4]

CASSCF and CASPT2 calculations were performed using MOLCAS 7.4 software,[5,6] and DFT and TD-DFT calculations using Gaussian 09 software.[7]

Table S2 The S1->S0 vertical energy (nm) of $\mathbf{2_{IPT}}$ for the optimized geometries in Cs symmetry

Geom-1 (1)				Geom-2 (2)	
TD(B3LYP)(3)	TD(CAM)(4)	CAS(5)	PT2(6)	CAS(5)	PT2(6)
879	544	709	551	1038	582

(1) Optimized geometry at TD(B3LYP)/6-31+G(d) (2) Optimized geometry at CASSCF(8,8)/ANO-L

(3) TD(B3LYP)/6-31+G(d) (4) TD(CAM-B3LYP)/6-31+G(d)

(5) 4-SA-CASSCF(10,10)/ANO-L (6) 4-SA-MS-CASPT2(10,10)/ANO-L

Evaluation of ESIPT emission energies by ONIOM method

The vertical S_1–S_0 energies in the crystalline polymorphs were computationally evaluated by means of ONIOM method,[8] a representative implementation of quantum mechanics and molecular mechanics (QM/MM). We performed two layer ONIOM calculations on the molecular clusters extracted from the three crystalline phases **2-Y**, **2-O**, and **2-R**, where one $\mathbf{2_{IPT}}$ species was immersed in the surrounding 16 $\mathbf{2_{Enol}}$ molecules which exist within 8 Å from the center of mass of the $\mathbf{2_{IPT}}$ species. The aggregation effects on the S_1–S_0 energies were hence taken into account through the DFT (one $\mathbf{2_{IPT}}$ species) and semiempirical PM3 (16 $\mathbf{2_{Enol}}$ species) interactions within the finite model. Intermolecular charge transfer excitation and excitonic effects across DFT-PM3 regions were ignored as well as crystal field effect exert from infinite electrostatic interactions. The cluster models for the three polymorphs were illustrated in Figure S4. The S_1 state of the center $\mathbf{2_{IPT}}$ was under full geometry optimization at TD(B3LYP)/6-31G(d) level with the geometries of the surrounding 16 fixed $\mathbf{2_{Enol}}$ molecules evaluated at PM3 level (TD(B3LYP)/6-31G(d):PM3).

The ESIPT emission energies were evaluated by single point calculations of $\mathbf{2_{IPT}}$, π-stacked $\mathbf{2_{IPT}}$-$\mathbf{2_{Enol}}$ dimers (Figure S5), the monomer high layer ONIOM model ($\mathbf{2_{IPT}}$ (TD(CAM-B3LYP)/6-31G(d))/16 $\mathbf{2_{Enol}}$ molecules (PM3)), and the dimer high layer ONIOM model (π-stacked $\mathbf{2_{IPT}}$-$\mathbf{2_{Enol}}$ (TD(CAM-B3LYP)/6-31G(d))/15 $\mathbf{2_{Enol}}$ molecules (PM3)).

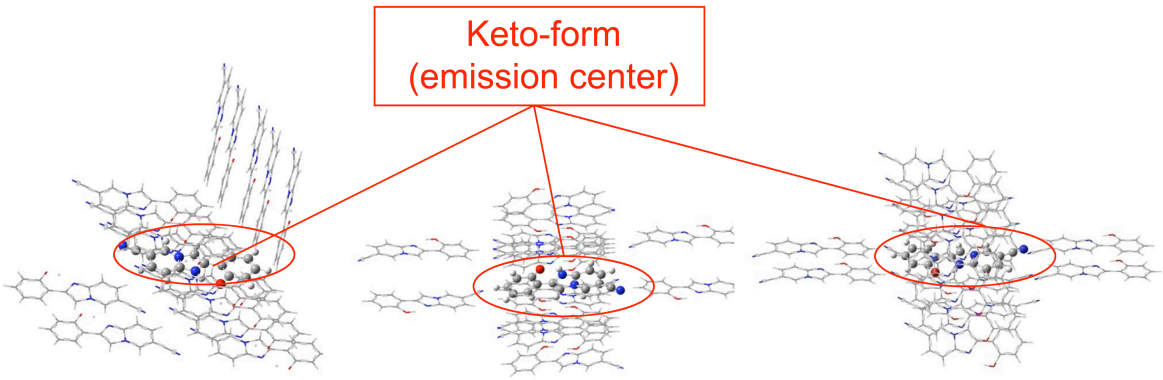

Figure S4. The ONIOM models for **2-Y**, **2-O** and **2-R**.

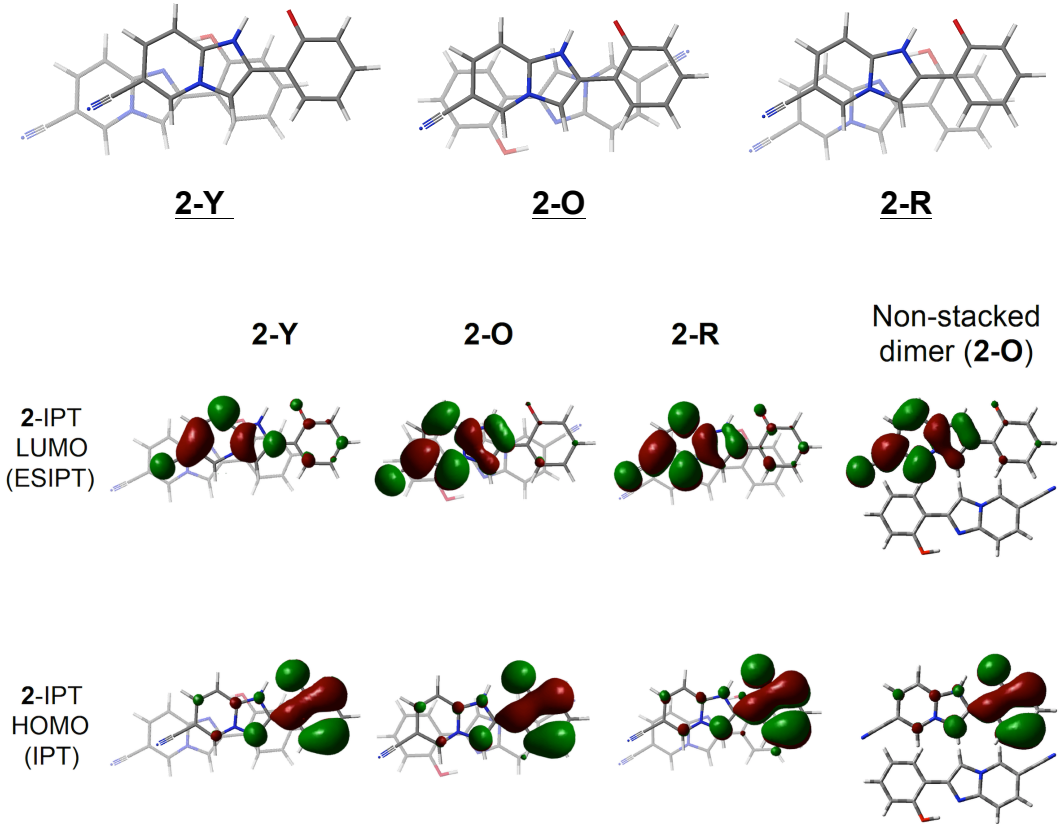

Figure S5. The central π-stacked dimers ($\mathbf{2}_{\mathbf{IPT}}$–$\mathbf{2}_{\mathbf{Enol}}$) (upper), and calculated HOMO and LUMO of **2-Y**, **2-O**, **2-R**, and non-stacked dimer (extracted from **2-O**) by TD(CAM-B3LYP)/6-31G(d) (lower).

References

1. Sheldrick, G. M., SHELX-97, Program for the Solution and Refinement of Crystal Structures, University of Göttingen, Germany, 1997.
2. T. Yanai, D. Tew, and N. Handy, *Chem. Phys. Lett.*, **2004**, *393*, 51-57.
3. Jacquemin, D.; Wathelet, V.; Perpète, E.A.; Adamo, C. *J. Chem. Theory Comput.* **2009**, 5, 2420–2435.
4. Jacquemin, D.; Wathelet, V.; Perpète, E.A.; Adamo, C. *Int. J. Quant. Chem.* 2010, *110*, 2121–2129.
5. MOLCAS ver.7.4, Lund University, 2008; Aquilante, F.; Vico, L.De.; Ferré, N.; Ghigo, G.; Målmqvist, P.-Å; Neogrády, P.; Pedersen, T.B.; Pitonak, M.; Reiher, M.; Roos, B.O.; Serrano-Andrés, L.; Urban, M.; Veryazov, V.; Lindh, R.; *J. Comput. Chem.*, **2010**, *31*, 224.
6. Widmark, P.-O.; Målqvist, P.-A.; Roos, B.O. *Theor. Chim. Acta*, **1990**, *77*, 291.
7. Frisch, M.J.; Trucks, G.W.; Schlegel, H.B.; Scuseria, G.E.; Robb, M.A.; Cheeseman, J.R.; Scalmani, G.; Barone, V.; Mennucci, B.; Peters-son, G.A.; Nakatsuji, H.; Caricato, M.; Li, X.; Hratchian, H.P.; Izmaylov, A.F.; Bloino, J.; Zheng, G.; Sonnenberg, J.L.; Hada, M.; Ehara, M.; Toyota, K.; Fukuda, R.; Hasegawa, J.; Ishida, M.; Nakajima, T.; Honda, Y.; Kitao, O.; Nakai, H.; Vreven, T.; Montgomery, Jr., J.A.; Peralta, J.E.; Ogliaro, F.; Bearpark,; Heyd, J.J.; Brothers, E.; Kudin, K.N.; Staroverov, V.N.; Kobayashi, R.; Normand, J.; Raghavachari, K.; Rendell, A.; Burant, J.C.; Iyengar, S.S.; Tomasi, J.; Cossi, M.; Rega, N.; Millam, J.M.; Klene, M.; Knox, J.E.; Cross, J.B.; Bakken, V.; Adamo, C.; Jaramillo, J.; Gomperts, R.; Stratmann, R.E.; Yazyev, O.; Austin, A.J.; Cammi, R.; Pomelli, C.; Ochterski, J.W.; Martin, R.L.; Morokuma, K.; Zakrzewski, V.G.; Voth, G.A.; Salvador, P.; Ortiz, J.V.; Cioslowski, J.; Fox, D.J.; Gaussian 09 revision B.1, Gaussian Inc. Wallingford CT 2009.
8. Dapprich, I. Komaromi, K.S. Byun, K. Morokuma, and M.J. Frisch. *J. Mol. Struc., THEOCHEM* 1999, *461-462*, 1.